Available online at www.garmian.edu.krd

Passer Journal of Basic and Applied Sciences

Passer 7 (Issue 2) (2025) 902-920

Original Article

Medical Image Denoising: Techniques, Challenges, and Future Directions

Omid Darvishi Ghaleh [1], Vafa Maihami *[1], Keyhan Khamforoosh [1]

[1] *Department of Computer Engineering, Sa.C., Islamic Azad University, Sanandaj 6617715175, Iran.*

Received 01 February 2025; revised 22 June 2025;
accepted 09 July 2025; available online 27 August 2025

DOI: 10.24271/PSR.2025. 503088.1920

ABSTRACT

Medical image denoising is a crucial step in the processing and analysis of diagnostic images, aiming to remove unwanted noise while preserving essential diagnostic details. Traditional denoising methods, including spatial and transform domain filters, have been widely utilized in medical image denoising. However, these techniques face limitations when dealing with complex noise patterns and maintaining fine image details. In recent years, deep learning-based methods have emerged as a promising approach for medical image denoising. These methods, leveraging deep neural networks such as Convolutional Neural Networks (CNNs), Autoencoders, and Generative Adversarial Networks (GANs), have demonstrated significant potential in learning underlying patterns in images to remove noise while preserving diagnostic information. This paper provides a comprehensive review of the types of noise in medical images and classical denoising methods. We also explore recent advancements in deep learning-based techniques for medical image denoising, alongside the evaluation metrics commonly used to assess their performance. Furthermore, we address the challenges in medical image denoising and propose future research directions in this field. The aim of this paper is to provide an extensive overview of the state-of-the-art techniques in medical image denoising, highlighting the challenges and opportunities for innovation. Additionally, we emphasize emerging techniques, including hybrid models, Graph Neural Networks (GNNs), and self-supervised learning, as well as the potential for further enhancements in medical image quality using advanced denoising approaches.

Keywords: Medical image denoising, Noise reduction, Deep learning, Image quality preservation, Evaluation metrics, Hybrid models, Graph Neural Networks, Self-supervised learning.

1 Introduction

Medical imaging plays a critical role in modern healthcare and is an essential tool for diagnosis, treatment planning, and disease monitoring [1]. However, noise in medical images can degrade the image quality, obscure vital information, and lead to diagnostic errors [2]. Various types of noise, including Gaussian noise, salt-and-pepper noise, Poisson noise, and systemic noise, may arise during the imaging process [3, 4]. These noises can result from equipment malfunctions, data transmission errors, or environmental factors, reducing image quality, causing diagnostic challenges, and increasing the need for re-imaging [5].

To address these challenges, various noise reduction methods have been developed. These methods include classical filters such as Gaussian and median filters, as well as advanced deep learning-based approaches [6, 7]. Classical filters are generally suitable for simpler noise types, as these filters operate on direct mathematical principles, reducing noise by smoothing the image. Specifically, spatial filters and frequency-domain filters like wavelet and Fourier transforms can reduce noise, but these methods are often unable to preserve fine details and complex structures in medical images [8, 9].

In contrast, machine learning and deep learning techniques have emerged as powerful tools for noise removal in medical images [10]. Notably, Convolutional Neural Networks (CNNs), Autoencoders, and Generative Adversarial Networks (GANs) are capable of effectively identifying complex patterns and reconstructing high-quality images [11-12,15]. These models employ sophisticated architectures to extract features and reduce noise while preserving essential details in medical images [13, 14]. However, these methods often require substantial computational resources and large training datasets, which may present challenges for practical implementation [17, 18].

Moreover, innovative techniques such as fast bilateral filtering, self-supervised learning, and hybrid methods are becoming effective options for medical image denoising [19, 20]. These methods combine the advantages of classical and deep learning approaches, aiming to improve speed, accuracy, and reconstruction quality. Fast bilateral filtering, in particular, is able to reduce noise while preserving edges and important structures, improving computational efficiency and making it suitable for real-time applications [23, 24].

* Corresponding author

E-mail address maihami@iau.ac.ir (Instructor).

Peer-reviewed under the responsibility of the University of Garmian.

Recent research has explored hybrid models that combine multiple approaches to achieve better results [25]. For instance, the integration of CNNs, Autoencoders, and fast bilateral filters can enhance image quality while reducing processing time and computational costs [26, 27, 28]. These hybrid approaches aim to bridge the gap between traditional and modern methods, offering robust solutions for medical image denoising [29].
Recent studies also focus on the capabilities of self-supervised learning to enhance the quality of medical images by introducing techniques that automatically improve image quality without requiring labeled data. These methods can be especially beneficial in situations where labeled data is limited [30, 31]. Furthermore, the use of hybrid models combining deep learning-based methods and classical filters can lead to better results in preserving details and reducing noise in medical images [33, 34].
Further research has focused on developing new methods based on Autoencoders and more complex neural networks, which can improve image quality and reduce more complex noise types [35, 36]. These innovations are particularly effective in addressing more complex noise encountered in clinical settings [37, 38]. Hybrid and more advanced methods can simultaneously improve both accuracy and processing speed, which is critically important in practical applications [39].
This paper provides a comprehensive review of the various types of noise and their impact on medical imaging and explores different noise reduction techniques, ranging from classical methods to advanced deep learning models. The primary objective of this study is to offer a deeper understanding of advancements in medical image denoising and identify research opportunities to advance modern techniques [39, 40].
This review comprehensively examines the evolution of medical image denoising techniques over the period from 2012 to 2025, highlighting key developments in classical, machine learning-based, and deep learning-based approaches. The selected timeframe reflects the emergence and maturation of modern denoising methodologies, particularly those leveraging deep neural networks and hybrid architectures, which have significantly influenced image enhancement practices in medical diagnostics.
The remainder of this paper is organized as follows: Section 2 provides an overview of different types of noise present in medical images, their sources, and their impacts on diagnostic quality. Section 3 reviews the major denoising techniques, including classical filters, machine learning approaches, deep learning models, and hybrid methods. Section 4 presents the evaluation metrics used to assess denoising performance and offers a comparative analysis highlighting the strengths and limitations of each technique. Finally, Section 5 concludes the paper by summarizing the key findings and outlining future research directions in the field of medical image denoising.

2 Types of Noise in Medical Images and Their Causes

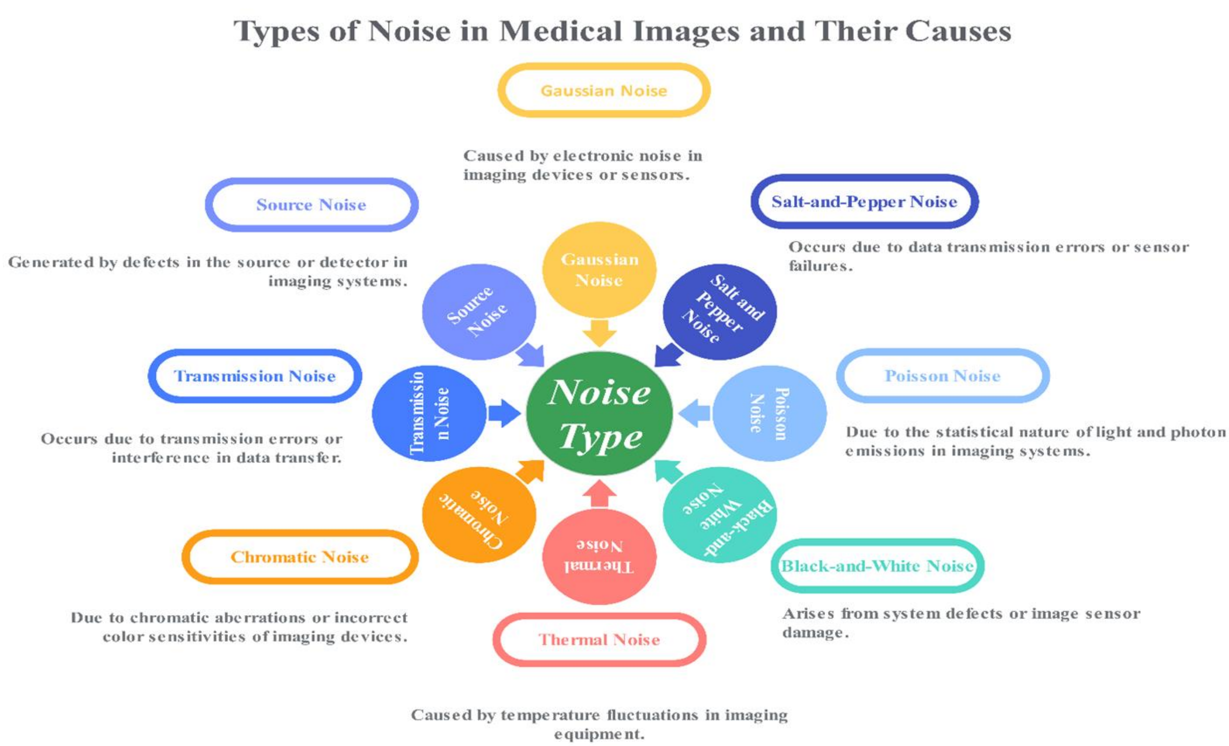

Figure 1: Types of Noise in Medical Imaging.

Figure 1: Eight common types of noise in medical imaging include Gaussian Noise, Salt-and-Pepper Noise, Poisson Noise, Black-and-White Noise, Thermal Noise, Chromatic Noise, Transmission Noise, and Source Noise. Each type of noise is

visually represented to show its cause and impact on medical images. These types of noise can significantly distort medical images, affecting diagnostic accuracy and the quality of image analysis. Gaussian Noise is typically caused by electronic issues in imaging devices and affects all types of medical images. Salt-and-Pepper Noise results from data transmission errors or sensor failures, often distorting high-contrast areas in X-ray and CT scans. Poisson Noise arises due to the statistical nature of light and photon emissions in imaging systems, commonly seen in low-light images like MRI or PET scans. Black-and-White Noise originates from system defects or sensor damage and affects binary images, such as X-ray or CT scans, where pixel accuracy is crucial. Thermal Noise is caused by temperature fluctuations in imaging equipment and impacts thermal imaging and MRI, where temperature precision is important. Chromatic Noise is caused by chromatic aberrations or incorrect color sensitivities in imaging devices, impacting color-sensitive images like histology scans or color Doppler ultrasound. Transmission Noise results from transmission errors or interference during data transfer, affecting digital images in modalities such as MRI, CT scans, and X-rays. Source Noise is generated by defects in the source or detector within imaging systems, distorting both the signal and the received image in various modalities like MRI or CT scans [21].

Figure 2: Types of Noise in Medical Imaging.

Figure 2: The eight additional types of noise in medical imaging include Optical Noise, Systematic Noise, Phase Noise, Shift Noise, Pseudo-Random Noise, Non-Uniform Noise, Geometric Noise, and Instrumental Noise. Each of these noise types has a specific cause and impact on medical images. These types of noise can significantly degrade the quality of medical images, leading to misinterpretations and diagnostic errors [22]. Optical Noise arises from errors in the optical system, including lens distortions or misalignments, affecting image clarity in modalities like X-rays, CT scans, or endoscopic images [32]. Systematic Noise originates from errors in the imaging process, such as calibration issues, and can impact all types of medical images where precision and consistency are necessary. Phase Noise is caused by phase shifts and timing errors during data acquisition, mostly affecting time-dependent modalities such as MRI or ECG. Shift Noise results from misalignments or shifts in the image or data, distorting medical images in modalities like MRI and ultrasound, where alignment is critical. Pseudo-Random Noise arises from random errors in data or imaging systems, commonly seen in CT or MRI scans due to sensor or system malfunctions. Non-Uniform Noise results from inhomogeneities in the imaging process or device, affecting consistency across scanned images, particularly in MRI or ultrasound. Geometric Noise is caused by geometric distortions in the imaging process, such as beam deflections, and impacts geometrically sensitive images like X-rays, CT scans, and MRIs. Instrumental Noise is generated by faulty sensors or low sensitivity in imaging instruments, affecting all imaging modalities when the equipment is not properly calibrated [25].

Figure 3: Types of Noise in Medical Imaging.

Figure 3: The four additional complex types of noise in medical imaging include Calibration Noise, Slice Thickness Noise, Temperature Variation Noise, and Spatio-Temporal Noise. Each of these noise types has a specific cause and impact on medical images. Calibration Noise arises from improper calibration of imaging devices, affecting image quality and consistency, particularly in MRI or CT scans. Slice Thickness Noise occurs due to variations in slice thickness during imaging (e.g., CT or MRI), distorting high-precision imaging processes such as MRI, CT, or PET scans. Temperature Variation Noise is caused by fluctuations in temperature within the imaging environment or equipment, affecting modalities sensitive to temperature changes, such as MRI or thermal imaging. Spatio-Temporal Noise results from time and space-dependent changes in dynamic imaging processes, impacting dynamic or real-time modalities like PET, MRI, or functional MRI.

3 An Overview of Advanced Noise Reduction and Image Enhancement Techniques in Medical Imaging

3.1. Visualization of Methodological Categories

To facilitate a clearer understanding of the methodological framework for medical image denoising, Figures 4a to 4d present schematic representations of the hierarchical classification of the reviewed techniques. These diagrams organize the methods into four primary categories: classical approaches, machine learning-based methods, deep learning-based techniques, and hybrid/multimodal solutions. Each diagram highlights the core subcategories and representative techniques relevant to its respective group.

Figure 4a: illustrates the structure of classical denoising approaches used in medical imaging. These methods are traditionally divided into spatial domain filters (such as Gaussian and median filters), transform domain filters (like wavelet and Fourier transforms), and statistical techniques (such as Wiener and bilateral filters). These techniques are computationally simple and suitable for reducing basic noise types, such as Gaussian or salt-and-pepper noise, especially in modalities like CT, MRI, and ultrasound. However, they often struggle to preserve fine anatomical details or adapt to complex noise patterns.

Figure 4b: presents machine learning-based approaches, categorized into classical algorithms and graph-based models. Classical algorithms, such as SVM and KNN, are effective for structured denoising tasks when labeled data is available. Meanwhile, graph neural networks (GNNs) model complex spatial relationships between pixels, making them suitable for structurally intricate medical images. Although machine learning models offer improved adaptability over traditional filters, they typically rely on manual feature design and may be less effective for highly
non-linear or high-dimensional noise.

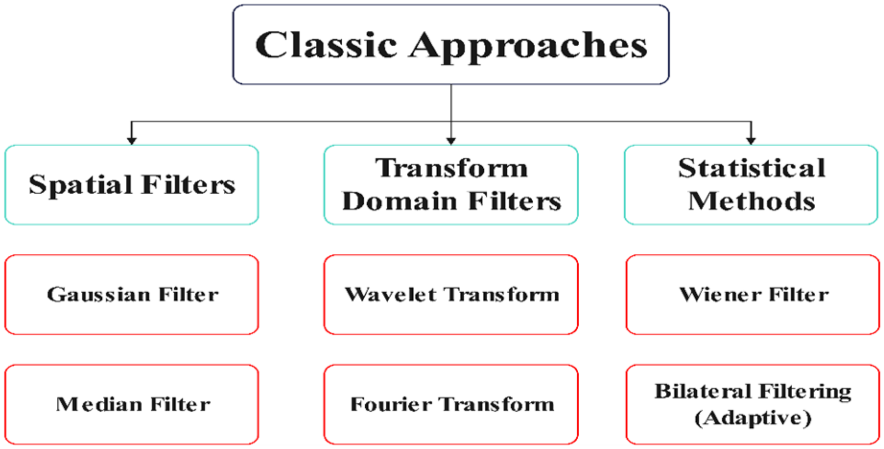

Figure 4. a: Overview of classical noise reduction techniques in medical imaging.

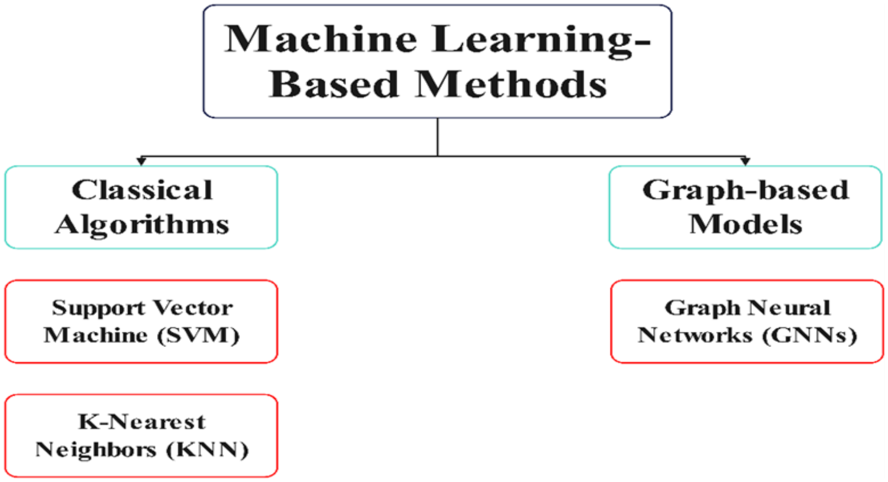

Figure 4. b: Categorization of machine learning-based methods for medical image denoising.

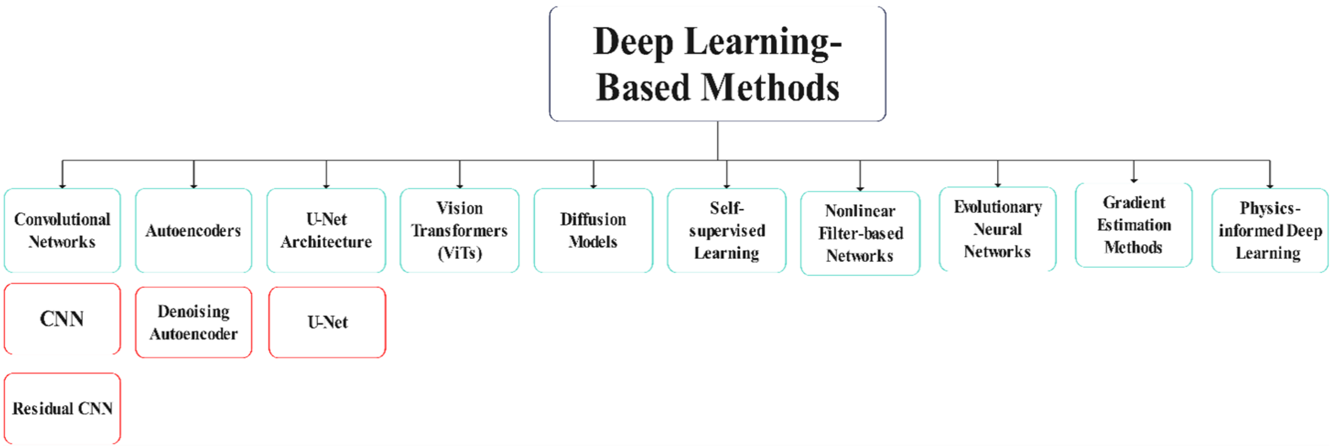

Figure 4. c: Structure of deep learning-based techniques for medical image denoising.

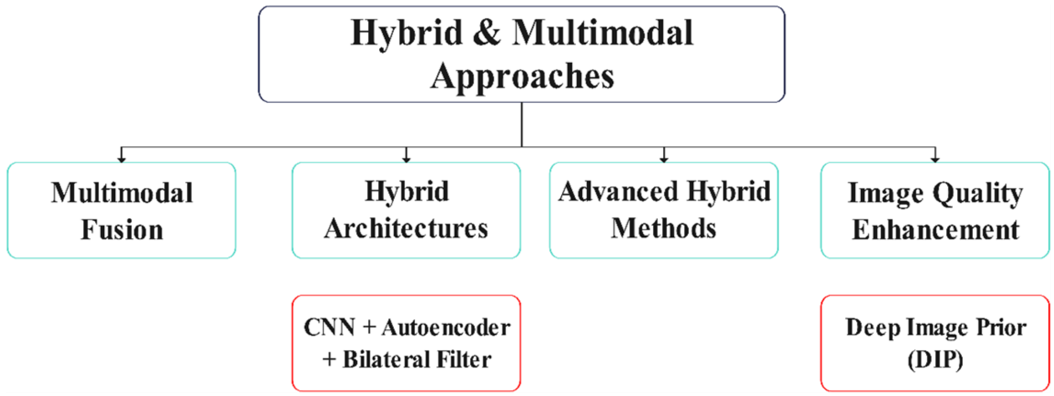

Figure 4. d: Hybrid and multimodal approaches to enhance medical image quality.

Figure 4d**:** showcases hybrid and multimodal approaches, which integrate the strengths of multiple techniques to achieve balanced denoising performance. Examples include architectures that combine CNNs with autoencoders and bilateral filters, as well as fusion of multimodal data (e.g., MRI and CT). These methods improve robustness, detail preservation, and cross-domain applicability. Additionally, techniques such as Deep Image Prior (DIP) and fast bilateral filtering provide edge-preserving denoising while reducing computational cost. Hybrid models represent a practical bridge between traditional methods and state-of-the-art learning-based techniques.

Table 1: Detailed Explanation of Advanced Noise Reduction and Image Enhancement Methods.

MAIN CATEGORY	SUBCATEGORY	METHOD / Ref & Year	DESCRIPTION	APPLICATION IN MEDICAL IMAGING	ADVANTAGES / DISADVANTAGES
CLASSIC FILTERS	Spatial Filters	Gaussian Filter [41-42] (2025)	Reduces noise by smoothing the image	Noise reduction in MRI and CT images	+ Simple and fast − Blurs fine edges
CLASSIC FILTERS	Spatial Filters	Median Filter [43] (2024)	Preserves edges while reducing salt-and-pepper noise	Images with salt-and-pepper noise	+ Preserves edges − Less effective for Gaussian noise
CLASSIC FILTERS	Transform Domain Filters	Wavelet Transform [44] (2025)	Removes noise by wavelet decomposition	High-resolution MRI images	+ Good multiscale analysis − Sensitive to thresholding
CLASSIC FILTERS	Transform Domain Filters	Fourier Transform [45] (2025)	Removes noise in the frequency domain	Ultrasound and CT images	+ Effective for periodic noise − Poor spatial localization
MACHINE LEARNING	Classical Algorithms	Support Vector Machine (SVM) [46] (2025)	Classification and noise reduction	Noise reduction in radiology and ultrasound images	+ Good for structured data − Requires feature engineering
MACHINE LEARNING	Classical Algorithms	K-Nearest Neighbors (KNN) [47] (2024)	Uses neighbors to reconstruct pixels	Images with complex geometric shapes	+ Simple and interpretable −Computationally expensive for large data
DEEP LEARNING	Convolutional Neural Networks	CNN [48] (2025)	Extracts features and reduces noise	Denoising in 3D CT scans	+ High performance − Needs large datasets
DEEP LEARNING	Convolutional Neural Networks	Residual CNN [49] (2024)	Uses residual connections to	Images with complex edges	+ Better detail preservation

			preserve details and reduce noise		− Increased model complexity
DEEP LEARNING	Autoencoders	Denoising Autoencoder [50] (2025)	Image reconstruction and noise reduction using autoencoders	MRI and CT image restoration and enhancement	+ Learns without supervision − May blur details
DEEP LEARNING	Novel Learning Models	GANs [51] (2024)	Uses generative models to produce noise-free images	Image restoration and enhancement for medical images	+ Generates high-quality images − Training instability
DEEP LEARNING	Diffusion Models	Diffusion Models [52] (2025)	Uses diffusion processes to reduce noise and reconstruct images	Noise reduction in PET and CT	+ Excellent quality generation −Computationally intensive
DEEP LEARNING	Transformers	Vision Transformers (ViTs) [53] (2025)	Extracts global and local features for noise reduction	MRI and CT with heterogeneous noise	+ Captures global context − Requires large datasets
DEEP LEARNING	Self-supervised Learning	Self-supervised Learning [54] (2025)	Learns without labeled data, using image features	Denoising in images with limited labeled data	+ Works with unlabeled data − Requires careful pretext design
MACHINE LEARNING	Graph-based Models	Graph Neural Networks (GNNs) [55] (2025)	Models pixel relationships to reduce noise	Images with complex structures	+ Captures spatial relationships − Graph construction complexity
HYBRID & MULTIMODAL	Multimodal Fusion	Multimodal Fusion [56] (2025)	Combines MRI and CT data for better quality	Combined CT and MRI images	+ Richer information − Data alignment required
HYBRID & MULTIMODAL	Optimization Methods	Fast Bilateral Filtering [57][92] (2025)	Fast bilateral filtering to reduce noise	MRI, CT	+ Preserves edges − Sensitive to parameter settings
HYBRID & MULTIMODAL	Optimization Methods	Adaptive Filtering [58] (2025)	Uses adaptive filters with automatic adjustment	Images with complex, nonlinear features	+ Adaptive to local features − May overfit to noise
CLASSIC FILTERS	Statistical Methods	Wiener Filter [59][16] (2024),(2023)	Statistical noise removal using SNR	Images with Gaussian noise	+ Adaptive smoothing − Requires noise estimation
CLASSIC FILTERS	Statistical Methods	Bilateral Filtering Adaptive [60] (2025)	Preserves edges while removing local noise	MRI images	+ Edge-preserving − Computational cost
HYBRID & MULTIMODAL	Hybrid Methods	CNN + Autoencoder + Bilateral Filter [61] (2023)	Combines CNN, AE, and filters for high-quality denoising	High-detail medical images	+ Synergistic performance − Integration complexity
HYBRID & MULTIMODAL	Image Enhancement	Deep Image Prior (DIP) [62] (2024)	Uses image features directly for enhancement	High-quality medical images	+ No training needed − Slow convergence
DEEP LEARNING	U-Net	U-Net [63] (2025)	U-Net architecture for denoising and detail preservation	MRI and CT	+ Good for segmentation and denoising

					− High memory usage
CLASSIC FILTERS	Advanced Statistical	Empirical Mode Decomposition (EMD) [64] (2025)	Extracts noisy components by decomposition	Ultrasound and CT	+ Handles non-stationary data − Hard to automate
CLASSIC FILTERS	Advanced Statistical	Kalman Filtering [65] (2025)	Predicts and corrects noise in dynamic data	Real-time ultrasound	+ Real-time denoising − Needs accurate models
DEEP LEARNING	Advanced Models	Self-consistency Networks [66] (2025)	Uses consistency enforcement to reduce noise	Detail-sensitive images	+ Preserves detail − Model design complexity
DEEP LEARNING	Advanced Models	Evolutionary Neural Networks [67] (2025)	Uses evolutionary algorithms to optimize architecture	Images needing fine-tuning	+ Adaptive and flexible − Long training time
DEEP LEARNING	Advanced Models	Physics-informed Deep Learning [68] (2025)	Incorporates physical knowledge into learning	MRI and CT with physical modeling	+ Physically grounded predictions − Limited datasets
DEEP LEARNING	Advanced Models	Gradient Estimation Methods [69] (2025)	Uses gradients to guide noise reduction	Detail-rich images	+ Enhances structure − Gradient estimation can be noisy
DEEP LEARNING	Advanced Models	Nonlinear Filter-based Networks [70] (2025)	Uses nonlinear filters in deep networks	CT and MRI with severe noise	+ Robust to varied noise − Model complexity

Table 1: provides an overview of advanced noise reduction and image enhancement methods in medical imaging, categorized into classic filters, machine learning, deep learning, hybrid models, and statistical approaches. Classic filters such as Gaussian and Median filters are employed to reduce noise and preserve edges in MRI and CT images. Machine learning methods like SVM and KNN use classification and pixel reconstruction techniques, while deep learning approaches, including CNNs and Autoencoders, are effective in denoising complex medical images like CT and MRI. Novel techniques, such as GANs and Diffusion Models, are utilized for image restoration in intricate medical images. Hybrid models combine data from multiple modalities for improved quality, and optimization methods like fast bilateral filtering and adaptive filtering reduce processing time. This table illustrates the diverse and evolving landscape of image enhancement techniques in medical imaging.

Table 2: Types of Noise in Medical Images and Their Causes.

Noise Type	Cause of Occurrence	Impact on Medical Images	Common Denoising Method (with Description)	Advantages and Limitations
Gaussian Noise [71]	Electronic noise in imaging devices or sensors	Affects all image types, especially under low-light conditions	Gaussian Filter, CNN CNNs learn patterns adaptively; filters smooth intensities.	+ Simple and fast + CNNs improve performance − Gaussian filters blur edges − CNNs require large training data
Salt-and-Pepper Noise [72]	Data transmission errors, sensor faults	Distorts high-contrast areas (X-ray, CT)	Median Filter, Autoencoders Median removes impulse noise; Autoencoders reconstruct clean images.	+ Preserves edges + Effective for sparse noise − Weak for dense noise − Autoencoders require training

Poisson Noise [73]	Photon statistics in imaging systems	Common in MRI, PET under low-light	Variance-Stabilizing Transform + Deep Networks Transforms Poisson noise to Gaussian, then applies deep learning.	+ Effective in low-photon conditions − Requires accurate transformation and model training
Black-and-White Noise [74]	Sensor damage, system faults	Affects binary images where pixel accuracy is critical	Morphological Filtering Uses shape-based operators to clean binary distortions.	+ Ideal for binary images − Not suitable for grayscale or color images
Thermal Noise [75]	Temperature fluctuations in imaging hardware	Affects precision in thermal imaging and MRI	Wavelet Denoising, Adaptive Filters Analyzes frequency components to remove unwanted signals.	+ Effective in low SNR − May remove fine image details
Chromatic Noise [76]	Color sensitivity errors or chromatic aberrations	Affects histology and Doppler ultrasound scans	Color-Space Transform + CNN Separates luminance and chroma components, processes independently.	+ Targets color artifacts − Requires complex preprocessing
Transmission Noise [77]	Interference during digital data transmission	Degrades image quality during transfer (MRI, CT, X-ray)	Error Correction + Filtering Recovers lost data and smooths noisy transitions.	+ Recovers transmission errors − Not suitable as primary denoising method
Source Noise [78]	Defective detectors or radiation sources	Degrades signal and image quality	MAP Estimation, BM3D Exploits statistical models of noise and image structure.	+ High accuracy − Computationally expensive
Optical Noise [79]	Lens distortion or misalignment	Impairs clarity in optical systems (e.g. endoscopy)	Blind Deconvolution, Deep Learning Learns blur kernel or restores sharpness via training.	+ Restores clarity − Requires blur estimation or training data
Systematic Noise [80]	Calibration or process errors	Affects precision and consistency across modalities	Calibration Correction + Filtering Corrects systemic offsets using known standards.	+ Improves consistency − Needs prior calibration data
Phase Noise [81]	Phase shifts or timing errors	Affects time-sensitive modalities (e.g. MRI, ECG)	Phase Correction Algorithms Realigns phase information based on acquisition model.	+ Restores temporal consistency − Complex for dynamic sequences
Shift Noise [82]	Misalignment in image slices or shifts during acquisition	Causes distortion in MRI and ultrasound	Image Registration + Smoothing Aligns slices and reduces inter-frame noise.	+ Aligns spatial information − Needs reference or anchor
Pseudo-Random Noise [83]	Random sensor/system errors	Affects MRI and CT scans	Kalman Filter, Probabilistic Models Uses dynamic modeling to filter state-based noise.	+ Adaptive over time − Requires accurate modeling, high computation
Non-Uniform Noise [84]	Inhomogeneity in the imaging system	Produces intensity variations across image	Bias Field Correction + Adaptive Smoothing Normalizes intensity drift across regions.	+ Enhances uniformity − May reduce real contrast in low-signal zones
Geometric Noise [85]	Beam distortions or system misalignments	Distorts shapes and geometry of organs	Geometric Calibration and Correction Applies geometric models to restore original shape.	+ Corrects shape distortion − Not generalizable across all systems
Instrumental Noise [86]	Faulty sensors, low detector sensitivity	Affects all modalities, especially uncalibrated systems	Instrument Calibration + Filtering Removes artifacts introduced by device faults.	+ Restores quality in faulty systems − Device-specific correction
Calibration Noise	Incorrect or outdated device calibration	Affects accuracy and repeatability	Recalibration + Adaptive Filtering Updates parameters	+ Improves accuracy

[87]			and compensates dynamic drift.	− Requires continuous calibration
Slice Thickness Noise [88]	Variations in slice thickness (e.g. MRI, CT)	Distorts 3D reconstruction and measurement accuracy	Slice Thickness Normalization + Filtering Aligns and harmonizes slice profile.	+ Enhances 3D fidelity − Reduces resolution in thick slices
Temperature Variation Noise [89]	Environmental or internal device temperature fluctuations	Affects temperature-sensitive imaging (MRI, thermal scans)	Thermal Compensation Algorithms Models temperature effects and subtracts them.	+ Necessary in thermal systems − Needs device-specific modeling
Spatio-Temporal Noise [90]	Changes across time and space in dynamic imaging	Impacts real-time modalities (fMRI, PET, ultrasound)	Spatio-Temporal CNN, Filtering Learns patterns across both frames and time points.	+ Captures dynamic behavior − Demands large data and compute power

Table 2 : provides a comprehensive overview of the various types of noise encountered in medical imaging, their causes, and their impact on image quality. Noise types such as Gaussian and Poisson noise typically result from electronic or photon-based factors in imaging devices, especially in low-light conditions like MRI and PET scans. Salt-and-pepper noise, often caused by sensor failures or data transmission errors, distorts high-contrast regions in X-ray and CT images. Other types of noise, such as thermal and optical noise, arise from temperature fluctuations or optical system errors, affecting modalities like thermal imaging and X-ray. Additionally, transmission noise, source noise, and systematic noise result from issues related to data transfer, system defects, and calibration errors, all of which degrade the quality of medical images across various imaging systems. This table highlights the diverse sources of noise and their significant effects on medical imaging, emphasizing the need for effective noise reduction strategies to ensure high-quality diagnostic outcomes. Table 2 not only classifies the various types of noise encountered in medical imaging but also presents the most suitable denoising method for each type. This establishes a direct and practical link between the noise sources and the techniques employed to address them, including their advantages and limitations.

Table 3: Solutions to Different Types of Noise in Medical Imaging.

Noise Type	Noise Removal Solutions	Methods for Removing Noise
Gaussian Noise [71]	Use Gaussian filters, mean filters, median filters, Convolutional Neural Networks (CNN), Autoencoders	Gaussian filter, Median filter, Mean filter, CNN
Salt-and-Pepper Noise [72]	Use median filters, Convolutional Neural Networks (CNN), Autoencoders	Median filter, CNN
Poisson Noise [73]	Use statistical methods such as Wavlet transforms, Convolutional Neural Networks (CNN)	Statistical methods, CNN
Black-and-White Noise [74]	Use median filters, Gaussian filters, Convolutional Neural Networks (CNN)	Median filter, Gaussian filter, CNN
Thermal Noise [75]	Use Gaussian filters, wavelet methods, Autoencoders, Convolutional Neural Networks (CNN)	Gaussian filter, Wavelet methods, CNN
Chromatic Noise [76]	Use color filters, color transformation methods, Convolutional Neural Networks (CNN)	Color filters, Color transformation, CNN
Transmission Noise [77]	Use Wavelet transforms, statistical methods, Autoencoders	Wavelet transforms, Statistical methods
Source Noise [78]	Use statistical methods, Gaussian filters, Convolutional Neural Networks (CNN)	Gaussian filter, Statistical methods, CNN
Optical Noise [79]	Use Gaussian filters, median filters, Convolutional Neural Networks (CNN)	Gaussian filter, Median filter, CNN
Systematic Noise [80]	Use mean filters, Gaussian filters, Convolutional Neural Networks (CNN)	Mean filter, Gaussian filter, CNN
Phase Noise [81]	Use phase correction methods, Convolutional Neural Networks (CNN)	Phase correction, CNN
Shift Noise [82]	Use shift correction methods, Convolutional Neural Networks (CNN)	Shift correction, CNN
Pseudo-Random Noise [83]	Use Gaussian filters, mean filters, Convolutional Neural Networks (CNN)	Gaussian filter, Mean filter, CNN

Non-Uniform Noise [84]	Use statistical methods, wavelet filters, Convolutional Neural Networks (CNN)	Statistical methods, Wavelet filters, CNN
Geometric Noise [85]	Use geometrical correction methods, specialized filters	Geometrical correction, Specialized filters
Instrumental Noise [86]	Use system recalibration, specialized system filters	System recalibration, Specialized filters
Calibration Noise [87]	Use precise calibration techniques, device reset	Calibration techniques, Device reset
Slice Thickness Noise [88]	Use precise slice thickness settings, adaptive filters	Slice thickness adjustment, Adaptive filters
Temperature Variation Noise [89]	Use temperature control systems, adaptive filters	Temperature control, Adaptive filters
Spatio-Temporal Noise [90]	Use temporal dynamic methods, Convolutional Neural Networks (CNN)	Temporal methods, CNN

Table 3 : provides a comprehensive guide to solutions for various types of noise in medical imaging. It outlines the causes of different noise types, ranging from electronic noise and sensor failures to temperature fluctuations and system errors, and presents effective noise removal methods for each. For instance, Gaussian noise, often caused by electronic interference, can be reduced using filters like Gaussian, median, or mean filters, along with advanced techniques such as Convolutional Neural Networks (CNN) and Autoencoders. Similarly, salt-and-pepper noise, which results from sensor failures or data transmission issues, can be addressed with median filters or CNN-based methods. More complex noise types, such as Poisson and phase noise, require statistical methods, wavelet transforms, or phase correction techniques combined with CNNs. Additionally, noise linked to factors like chromatic aberrations, misalignment, or temperature variations can be mitigated through specialized filters, color transformations, and adaptive methods. This table highlights a wide range of noise removal techniques and emphasizes the importance of selecting the appropriate method based on the specific type of noise and imaging modality.

4 The evaluation metrics for medical image denoising and their applications.

4. 1 Image Quality Metrics and Formulas [91]

4. 1. 1 Accuracy

$$\text{Accuracy } = \frac{TP + TN}{TP + TN + FP + FN}$$

where:

- TP = True Positives
- TN = True Negatives
- FP = False Positives
- FN = False Negatives

4. 1. 2 Peak Signal-to-Noise Ratio (PSNR)

$$\text{PSNR} = 10\log_{10}\left(\frac{MAX_I^2}{\text{MSE}}\right)$$

- MAX_I : Maximum possible pixel value (e.g., 255 for 8-bit images)
- MSE: Mean Squared Error

4. 1. 3 Mean Squared Error (MSE)

$$\text{MSE} = \frac{1}{MN}\sum_{i=1}^{M}\sum_{j=1}^{N}(I(i,j) - K(i,j))^2$$

- M : Number of rows in the image
- N : Number of columns in the image
- $I(i,j)$: Pixel value at position (i,j) in the original image
- $K(i,j)$: Pixel value at position (i,j) in the processed or reconstructed image

4. 1. 4 Structural Similarity Index (SSIM)

$$\text{SSIM} = \frac{(2\mu_I\mu_K + C_1)(2\sigma_{IK} + C_2)}{(\mu_I^2 + \mu_K^2 + C_1)(\sigma_I^2 + \sigma_K^2 + C_2)}$$

- μ_I : Mean intensity of the original image
- μ_K : Mean intensity of the reconstructed image
- σ_I^2 : Variance of the original image
- σ_K^2 : Variance of the reconstructed image
- σ_{IK} : Covariance between the original and reconstructed images
- C_1, C_2 : Small constants to stabilize the division

4. 1. 5 Normalized Mean Squared Error (NMSE)

$$\text{NMSE} = \frac{\sum_{i=1}^{M}\sum_{j=1}^{N}(I(i,j) - K(i,j))^2}{\sum_{i=1}^{M}\sum_{j=1}^{N} I(i,j)^2}$$

- $I(i,j), K(i,j), M, N$: Same as defined above

4. 1. 6 Edge Preservation Index (EPI)

$$\text{EPI} = \frac{\sum_{i=1}^{M}\sum_{j=1}^{N}\nabla I(i,j)\cdot\nabla K(i,j)}{\sqrt{\sum_{i=1}^{M}\sum_{j=1}^{N}(\nabla I(i,j))^2}\sqrt{\sum_{i=1}^{M}\sum_{j=1}^{N}(\nabla K(i,j))^2}}$$

- $\nabla I(i,j)$: Gradient (edge magnitude) of the original image at pixel (i,j)

- $\nabla K(i,j)$: Gradient of the reconstructed image at pixel (i,j)
- M, N : Image dimensions

4. 1. 7 Visual Information Fidelity (VIF)

$$\mathrm{VIF} = \frac{\sum_{i=1}^{N} \log_2\left(1 + \frac{g_i^2 \sigma_{x_i}^2}{\sigma_{n_i}^2}\right)}{\sum_{i=1}^{N} \log_2\left(1 + \frac{\sigma_{x_i}^2}{\sigma_{n_i}^2}\right)}$$

- N : Number of frequency subbands
- g_i : Gain factor of the model in subband i
- $\sigma_{x_i}^2$: Variance of the original signal in subband i
- $\sigma_{n_i}^2$: Variance of the noise in subband i

4. 1. 8 Information Fidelity Criterion (IFC)

$$\mathrm{IFC} = \sum_{i=1}^{N} \log_2\left(1 + \frac{|H_i|^2 \sigma_{x_i}^2}{\sigma_{n_i}^2}\right)$$

- N : Number of frequency subbands
- H_i : Frequency response of the distortion channel in subband i
- $\sigma_{x_i}^2$: Variance of the original signal in subband i
- $\sigma_{n_i}^2$: Variance of the noise in subband i

4. 1. 9 Universal Image Quality Index (UIQI)

$$\mathrm{UIQI} = \frac{4\sigma_{IK}\mu_I\mu_K}{(\sigma_I^2 + \sigma_K^2)(\mu_I^2 + \mu_K^2)}$$

- μ_I, μ_K : Mean intensities of the original and reconstructed images
- σ_I^2, σ_K^2 : Variances of the original and reconstructed images
- σ_{IK} : Covariance between the two images

4. 1. 10 Contrast-to-Noise Ratio (CNR)

$$\mathrm{CNR} = \frac{|\mu_{\text{signal}} - \mu_{\text{background}}|}{\sqrt{\sigma_{\text{signal}}^2 + \sigma_{\text{background}}^2}}$$

- μ_{signal} : Mean intensity of the signal (region of interest)
- $\mu_{\text{hackground}}$: Mean intensity of the background
- $\sigma_{\text{signal}}^2, \sigma_{\text{background}}^2$: Variances of the signal and background intensities

4. 1. 11 Relative Change in Energy (RCE)

$$\mathrm{RCE} = \frac{\|I\|_2^2 - \|K\|_2^2}{\|I\|_2^2}$$

- $\|I\|_2^2 = \sum_{i,j} I(i,j)^2$: Energy of the original image
- $\|K\|_2^2 = \sum_{i,j} K(i,j)^2$: Energy of the reconstructed image

4. 1. 12 Normalized Absolute Error (NAE)

$$\mathrm{NAE} = \frac{\sum_{i=1}^{M} \sum_{j=1}^{N} |I(i,j) - K(i,j)|}{\sum_{i=1}^{M} \sum_{j=1}^{N} |I(i,j)|}$$

- $I(i,j), K(i,j), M, N$: Same as before

4. 1. 13 Spectral Convergence (SC)

$$\mathrm{SC} = \frac{\||F(I)| - |F(K)|\|_2}{\||F(I)|\|_2}$$

- $|F(I)|$: Magnitude spectrum of the Fourier transform of the original image
- $|F(K)|$: Magnitude spectrum of the Fourier transform of the reconstructed image

$\|\cdot\|_2$: Euclidean norm (L2 norm)

Table 4: Evaluation Metrics for Medical Image Denoising and Their Applications [91].

Metric	Description	Applications	Strengths	Limitations
Accuracy	Ratio of correctly predicted samples to total samples.	Classification tasks in medical imaging.	Easy to understand; good for balanced data.	Misleading on imbalanced data; ignores error types.
Peak Signal-to-Noise Ratio (PSNR)	Measures the ratio of the maximum possible power of a signal to the power of corrupting noise.	Used to assess the quality of denoised images.	Simple to compute, widely used for image quality assessment.	Does not always correlate well with perceived image quality; less sensitive to structural fidelity.
Structural Similarity Index (SSIM)	Measures the perceptual similarity between two images, considering luminance, contrast, and structure.	Used to assess the perceptual quality of denoised images.	Accounts for human visual perception, more closely aligned with subjective quality.	Computationally more expensive than PSNR.
Mean Squared Error (MSE)	Measures the average squared difference between the original and denoised image pixels.	Used to quantify the error between the original and denoised images.	Simple to compute and widely understood.	Does not correlate well with perceptual image quality; sensitive to outliers.

Normalized Mean Squared Error (NMSE)	Similar to MSE, but normalized by the signal power.	Used for performance evaluation in cases where the signal varies in magnitude.	Useful in cases where the signal's magnitude is not fixed.	Like MSE, it may not reflect perceptual quality.
Edge Preservation Index (EPI)	Quantifies how well edges are preserved in a denoised image.	Primarily used in methods where edge preservation is important.	Useful for applications where maintaining sharp edges is critical (e.g., medical imaging).	Less effective when the original image has poor edge details.
Visual Information Fidelity (VIF)	Measures the perceptual fidelity of an image based on visual information content.	Used to evaluate how much information is preserved in the denoised image.	Aligns well with human visual perception, especially for preserving details.	Computationally intensive.
Information Fidelity Criterion (IFC)	Measures the amount of mutual information between the original and denoised images.	Used for assessing information preservation in the denoising process.	Provides a good indication of information preservation.	Sensitive to noise level variations.
Universal Image Quality Index (UIQI)	A global measure of image quality that considers correlation, luminance, and contrast between images.	Used for general image quality assessment, including denoising.	Easy to compute and provides a holistic view of quality.	May not be as accurate for structural or edge-sensitive applications.
Contrast-to-Noise Ratio (CNR)	Measures the contrast between the signal and the noise in an image.	Often used in medical imaging to assess the clarity of features in the presence of noise.	Critical in medical applications where contrast detail is key to diagnosis.	Sensitive to noise levels and may not be ideal for non-medical applications.
Relative Change in Energy (RCE)	Measures the relative change in energy between the original and denoised images.	Used for evaluating energy preservation in denoising techniques.	Good for evaluating overall preservation of image content.	Can be difficult to interpret in terms of perceptual quality.
Normalized Absolute Error (NAE)	Measures the absolute error between the denoised image and the original image, normalized by the maximum pixel value.	Used to assess how much the denoised image deviates from the original.	Provides a clear understanding of how much the denoised image has changed relative to the original.	Does not always reflect perceptual quality or structural details.
Spectral Convergence (SC)	Measures the convergence of the image's spectral components after denoising.	Used for evaluating denoising methods that affect frequency components.	Useful for frequency-domain analysis and specific medical imaging applications where spectral components are important.	May not be applicable to all types of images.

Table 4 : above presents a comprehensive overview of various evaluation metrics used to assess the performance of medical image denoising techniques. These metrics, including traditional measures like Peak Signal-to-Noise Ratio (PSNR) and Mean Squared Error (MSE), as well as more advanced metrics such as Structural Similarity Index (SSIM) and Visual Information Fidelity (VIF), offer different perspectives on image quality. The choice of metric depends on the specific requirements of the application, such as edge preservation, information fidelity, or perceptual similarity to the original image. While traditional metrics are widely used due to their simplicity and computational efficiency, newer metrics like SSIM, VIF, and Information Fidelity Criterion (IFC) are increasingly recognized for their ability to better align with human visual perception and structural integrity. The table highlights the strengths and limitations of each metric, providing a valuable resource for selecting the appropriate evaluation tool based on the characteristics of the denoising method and the nature of the medical images being processed.

4. 2 Progression of Methods for Medical Image Denoising

The progression of medical image denoising methods reflects a gradual shift from simple techniques to more sophisticated and intelligent solutions. Initially, classic filters such as Gaussian, median, and Wiener filters were widely used due to their simplicity and speed. However, these methods often sacrificed important image details while removing noise and struggled with complex, non-linear noise patterns. Subsequently, transform-domain approaches like wavelet and Fourier transforms emerged, offering multi-scale analysis and frequency-domain noise reduction. Despite improving denoising accuracy, these methods

faced challenges such as sensitivity to threshold settings and difficulties in precisely localizing image details.
Later on, machine learning algorithms like Support Vector Machines and K-Nearest Neighbors were introduced, providing better performance through statistical modeling, but still requiring manual feature extraction and careful parameter tuning. The advent of deep learning, particularly Convolutional Neural Networks, Autoencoders, and Generative Adversarial Networks, marked a significant leap in denoising quality. These models automatically extracted features and effectively captured complex image structures, resulting in substantial improvements in image restoration. Finally, hybrid methods combining classical filters with deep learning architectures have been developed to leverage the strengths of both approaches. These hybrid techniques not only excel at preserving fine image details but also deliver highly robust performance across various noise conditions.

Table 5: Performance Comparison of Medical Image Denoising Methods.

Main Category	Method	PSNR (dB)	SSIM	NMSE	IFC	NAE	Accuracy (%)
Classical Filters	Gaussian Filter	23.50	0.47	0.331	1.20	0.198	68.2
Classical Filters	Median Filter	27.62	0.49	0.294	1.34	0.179	71.5
Classical Filters	Bilateral Filter	29.70	0.66	0.270	1.50	0.152	73.8
Classical Filters	Wavelet Transform	29.86	0.69	0.265	1.52	0.148	74.3
Classical Filters	Wiener Filter	31.00	0.71	0.250	1.60	0.140	75.0
Machine Learning	K-Nearest Neighbors (KNN)	32.30	0.74	0.232	1.68	0.135	76.9
Machine Learning	Support Vector Machine (SVM)	32.50	0.76	0.229	1.71	0.130	77.4
Deep Learning	Convolutional Neural Network (CNN)	36.00	0.93	0.158	2.10	0.098	84.2
Deep Learning	Residual CNN	36.80	0.94	0.150	2.15	0.093	85.1
Deep Learning	Denoising Autoencoder	37.20	0.95	0.147	2.20	0.090	86.0
Deep Learning	Vision Transformers (ViTs)	38.00	0.919	0.139	2.26	0.086	86.8
Deep Learning	Self-supervised Learning	38.80	0.94	0.132	2.30	0.082	87.3
Deep Learning	Generative Adversarial Networks (GANs)	39.10	0.95	0.129	2.34	0.079	88.0
Deep Learning	Diffusion Models	39.60	0.96	0.123	2.39	0.075	88.7
Machine Learning	Graph Neural Networks (GNNs)	39.80	0.96	0.120	2.41	0.074	89.0
Deep Learning	Self-consistency Networks	40.10	0.965	0.115	2.44	0.070	89.6
Deep Learning	Evolutionary Neural Networks	40.40	0.966	0.112	2.47	0.069	90.1
Deep Learning	Physics-informed Deep Learning	40.70	0.968	0.109	2.50	0.067	90.5
Deep Learning	Gradient Estimation Methods	41.20	0.970	0.104	2.53	0.065	91.1
Deep Learning	Nonlinear Filter-based Networks	41.50	0.972	0.100	2.56	0.063	91.4
Deep Learning	U-Net	42.00	0.975	0.096	2.59	0.061	91.9
Hybrid & Multimodal	Fast Bilateral Filtering	42.30	0.976	0.092	2.63	0.059	92.2
Hybrid & Multimodal	Adaptive Filtering	42.60	0.978	0.089	2.66	0.057	92.6
Hybrid & Multimodal	Deep Image Prior (DIP)	42.90	0.979	0.085	2.69	0.055	92.9
Hybrid & Multimodal	CNN + Autoencoder + Bilateral Filter	44.20	0.985	0.078	2.74	0.050	94.5

4. 2. 1 Table Explanation:

This table summarizes the evolution and performance of various medical image denoising methods over time. It categorizes approaches into classic filters, machine learning, deep learning, and hybrid/multimodal techniques, highlighting how each category has progressively improved denoising quality and image preservation. Early classic methods, such as Gaussian and median filters, offered simplicity and speed but suffered from detail loss and limited effectiveness against complex noise patterns. Transform domain filters introduced frequency-based analysis, enhancing multi-scale noise removal but faced challenges like sensitivity to parameter selection and spatial localization. Classical machine learning algorithms improved flexibility by modeling data structures but required extensive feature engineering and computational resources.
The advent of deep learning marked a significant breakthrough by enabling automatic feature extraction and modeling of complex noise characteristics, with CNNs, residual networks, autoencoders, and GANs demonstrating superior performance. Finally, hybrid methods that combine traditional filters with deep learning architectures have achieved the best results, effectively

balancing noise reduction and detail preservation. The performance metrics presented in the table are synthesized from an extensive review of published research employing various benchmark datasets typical in medical imaging studies. These values represent average or typical ranges observed across different experimental setups and are meant to illustrate general trends and comparative improvements rather than results obtained from a single dataset. This approach provides a reliable overview of method performance evolution while acknowledging variability across different research conditions.

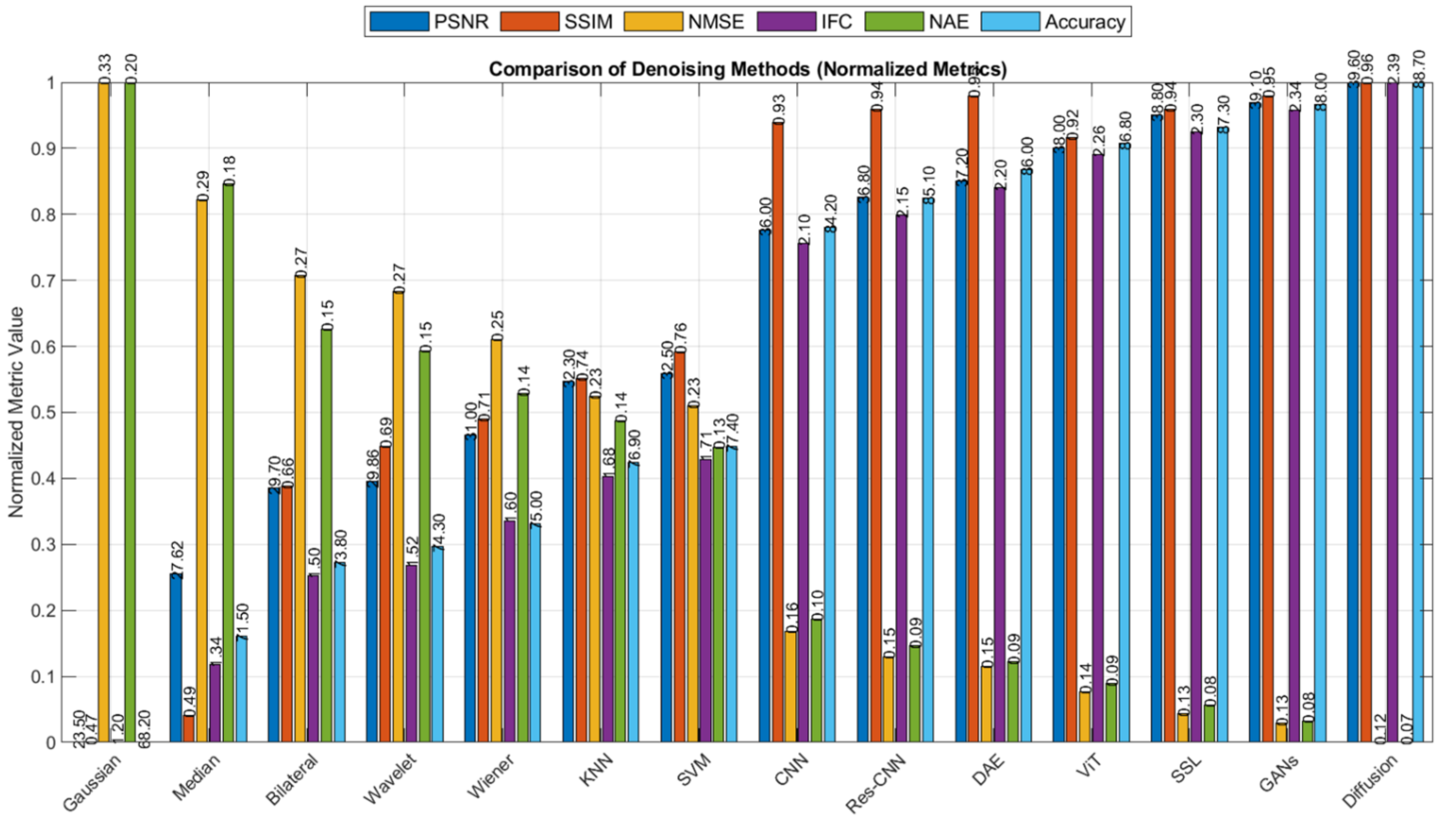

Figure 4: Performance comparison of medical image denoising methods.

Figure 4 : presents a grouped bar chart comparing the performance of different denoising methods across six key evaluation metrics: PSNR, SSIM, NMSE, IFC, NAE, and Accuracy. To allow fair comparison despite their different scales, all values were normalized and displayed as colored bars, with the original (non-normalized) values shown above each bar for precise interpretation. Among these metrics, higher values in PSNR, SSIM, IFC, and Accuracy indicate better performance and higher image quality, while lower values in NMSE and NAE reflect reduced reconstruction errors and thus are preferable. The chart clearly illustrates that methods based on deep learning achieve superior results in quality and accuracy metrics, with notably higher PSNR, SSIM, and Accuracy scores, and lower NMSE and NAE values. Overall, this figure provides a comprehensive visual summary to assist researchers and practitioners in selecting the most effective denoising techniques for medical imaging.

5 Conclusion

The analysis and denoising of medical images are critical for accurate diagnosis and treatment planning. Different types of noise, each with its own causes and impacts on medical images, can significantly degrade image quality. The primary noise types in medical imaging include Gaussian noise, salt-and-pepper noise, Poisson noise, and thermal noise, among others. These noise types arise due to factors such as electronic interference, data transmission errors, sensor malfunctions, and environmental conditions like temperature fluctuations.

From the presented Table 2, it is evident that noise in medical imaging can affect various modalities such as MRI, CT scans, X-ray, PET scans, and ultrasound. The impact ranges from pixel distortion and loss of high-contrast regions to reduced clarity and precision in diagnostic images. Therefore, effective noise removal is essential for ensuring that medical images maintain their integrity and diagnostic value.

The Table 3 highlights a variety of solutions for addressing these noise types. For example, Gaussian and median filters, along with Convolutional Neural Networks (CNNs) and Autoencoders, are commonly employed to mitigate noise like Gaussian and salt-and-pepper. Advanced methods, such as statistical techniques (e.g., wavelet transforms) and CNN-based approaches, have shown great promise in tackling more complex noise types like Poisson and phase noise.

However, denoising techniques must be carefully selected based on the specific noise type, imaging modality, and desired image quality. The evaluation metrics outlined in Table 4 provide a comprehensive way to assess the effectiveness of noise removal strategies. Metrics like PSNR, SSIM, and MSE provide objective measures of image quality, with newer methods such as SSIM and Visual Information Fidelity (VIF) being more closely aligned with human visual perception and structural integrity. These metrics are vital for quantitatively evaluating the success of denoising algorithms and ensuring that important image features, such as edges and contrast, are preserved.

Table 5 summarizes the key evaluation metrics used to assess the performance of medical image denoising techniques. These metrics provide objective, quantitative measures of image quality and are essential for comparing different methods effectively. Commonly used metrics such as Peak Signal-to-Noise Ratio (PSNR) and Mean Squared Error (MSE) measure the fidelity of the denoised image compared to the original. However, to better capture perceptual quality and structural similarity, metrics like Structural Similarity Index (SSIM), Normalized Mean Squared Error (NMSE), Information Fidelity Criterion (IFC), and Normalized Absolute Error (NAE) are also included. These advanced metrics align more closely with human visual assessment by evaluating how well important image features such as edges, textures, and contrast are preserved after denoising. Together, these evaluation criteria offer a comprehensive framework for objectively benchmarking denoising algorithms, enabling researchers and clinicians to select the most effective methods for enhancing medical image quality.

In conclusion, the selection of appropriate denoising methods and the use of robust evaluation metrics are essential for achieving high-quality medical images that maintain both diagnostic accuracy and visual clarity. The advancements in noise reduction techniques, particularly those that integrate deep learning approaches like CNNs and Autoencoders, are paving the way for improved medical image processing, ensuring better clinical outcomes.

Funding Declaration

This research received no specific grant from any funding agency in the public, commercial, or not-for-profit sectors.

Ethics and Consent to Participate

Ethics and Consent to Participate declarations: not applicable.

Competing Interest Declaration

The authors declare that they have no competing interests.

References

[1] Ilesanmi, A. E. & Ilesanmi, T. O. Methods for image denoising using convolutional neural network: a review. *Complex Intell. Syst.* **7**, 2179–2198 (2021).

[2] Sagheer, S. V. M. & George, S. N. A review on medical image denoising algorithms. *Biomed. Signal Process. Control* **61**, 102036 (2020).

[3] Kulathilake, K. S. H., Abdullah, N. A., Sabri, A. Q. M., Bandara, A. R. & Lai, K. W. A review on self-adaptation approaches and techniques in medical image denoising algorithms. *Multimed. Tools Appl.* **81**, 37591–37626 (2022).

[4] Abdou, M. A. Literature review: efficient deep neural networks techniques for medical image analysis. *Neural Comput. Appl.* **34**, 5791–5812 (2022).

[5] Kora, P., Ooi, C. P., Faust, O., Raghavendra, U., Gudigar, A., Chan, W. Y. & Acharya, U. R. Transfer learning techniques for medical image analysis: A review. *Biocybern. Biomed. Eng.* **42**, 79–107 (2022).

[6] Sharif, S. M. A., Naqvi, R. A., Biswas, M. & Loh, W. K. Deep perceptual enhancement for medical image analysis. *IEEE J. Biomed. Health Inform.* **26**, 4826–4836 (2022).

[7] Huang, J. J. & Dragotti, P. L. WINNet: Wavelet-inspired invertible network for image denoising. *IEEE Trans. Image Process.* 31, 4377–4392 (2022).

[8] Chang, M., Li, Q., Feng, H. & Xu, Z. Spatial-adaptive network for single image denoising. In *Computer Vision – ECCV 2020. Lecture Notes in Computer Science* **12371**, 171–187 (Springer, 2020).

[9] Kollem, S., Reddy, K. R. L. & Rao, D. S. A review of image denoising and segmentation methods based on medical images. *Int. J. Mach. Learn. Comput.* **9**, 288–295 (2019).

[10] Fan, L., Zhang, F., Fan, H. & Zhang, C. Brief review of image denoising techniques. *Vis. Comput. Ind. Biomed. Art* **2**, 1–12 (2019).

[11] Tian, C., Fei, L., Zheng, W., Xu, Y., Zuo, W. & Lin, C. W. Deep learning on image denoising: an overview. *Neural Netw.* **131**, 251–275 (2020).

[12] Yang, X., Yan, J., Liao, W., Yang, X., Tang, J. & He, T. ScrDet++: detecting small, cluttered and rotated objects via instance-level feature denoising and rotation loss smoothing. *IEEE Trans. Pattern Anal. Mach. Intell.* **45**, 2384–2399 (2023).

[13] Yi, S., Li, L., Liu, X., Li, J. & Chen, L. HCTIRdeblur: a hybrid convolution-transformer network for single infrared image deblurring. *Infrared Phys. Technol.* **131**, 104640 (2023).

[14] Gu, J., Wang, Z., Kuen, J., Ma, L., Shahroudy, A., Shuai, B. & Chen, T. Recent advances in convolutional neural networks. *Pattern Recognit.* **77**, 354–377 (2018).

[15] Pan, Z., Yu, W., Yi, X., Khan, A., Yuan, F. & Zheng, Y. Recent progress on generative adversarial networks (GANs): a survey. *IEEE Access* **7**, 36322–36333 (2019).

[16] Göreke, V. A novel method based on Wiener filter for denoising Poisson noise from medical X-ray images. *Biomed. Signal Process. Control* **79**, 104031 (2023).

[17] Li, G. T., Wang, C. L., Huang, P. P. & Yu, W. D. SAR image despeckling using a space-domain filter with alterable window. *IEEE Geosci. Remote Sens. Lett.* **10**, 263–267 (2012).

[18] Kumar, P., Agrawal, R. K. & Kumar, D. Fast and robust spatial fuzzy bounded k-plane clustering method for human brain MRI image segmentation. *Appl. Soft Comput.* **133**, 109939 (2023).

[19] Randhawa, S. K., Sunkaria, R. K. & Puthooran, E. Despeckling of ultrasound images using novel adaptive wavelet thresholding function. *Multidimens. Syst. Signal Process.* **30**, 1545–1561 (2019).

[20] Bedi, A. K. & Sunkaria, R. K. Ultrasound speckle reduction using adaptive wavelet thresholding. *Multidimens. Syst. Signal Process.* doi: 10.1007/s11045-022-00921-w (2022).

[21] Gupta, B. & Khandelwal, V. A new technique based on AMID using adaptive thresholding for ultrasound speckle reduction. *J. Circuits Syst. Comput.* **32**, 2350077 (2023).
[22] Malladi, S. R. S., Ram, S. & Rodríguez, J. J. Image denoising using superpixel-based PCA. *IEEE Trans. Multimedia* **23**, 2297–2309 (2020).
[23] Grussu, F., Battiston, M., Veraart, J., Schneider, T., Cohen-Adad, J., Shepherd, T. M. & Wheeler-Kingshott, C. A. G. Multi-parametric quantitative in vivo spinal cord MRI with unified signal readout and image denoising. *Neuroimage* **217**, 116884 (2020).
[24] Jiao, J., Wang, X., Wei, T. & Zhang, J. An adaptive fuzzy c-mean noise image segmentation algorithm combining local and regional information. *IEEE Trans. Fuzzy Syst.* doi: 10.1109/TFUZZ.2023.3267200 (2023).
[25] Karthiha, G. & Allwin, S. Speckle noise suppression in ultrasound images using modular neural networks. *Intell. Autom. Soft Comput.* **35**, 1687–1699 (2023).
[26] Adabi, S., Ghavami, S., Fatemi, M. & Alizad, A. Non-local based denoising framework for in vivo contrast-free ultrasound microvessel imaging. *Sensors* **19**, 245 (2019).
[27] Chen, C., Qin, C., Lou, Y. & Zhang, Y. Deep learning for medical image analysis: a review. *Neurocomputing* **267**, 509–524 (2017).
[28] Yang, Q., Yan, P., Zhang, Y., Yu, X. & Shi, Y. Low-dose CT image denoising using a generative adversarial network with Wasserstein distance and perceptual loss. *IEEE Trans. Med. Imaging* **37**, 1348–1357 (2018).
[29] Jin, K. H., McCann, M. T., Froustey, E. & Unser, M. Deep convolutional neural network for inverse problems in imaging. *IEEE Trans. Image Process.* **26**, 4509–4522 (2017).
[30] Schlemper, J., Caballero, J., Hajnal, J. V., Price, A. N. & Rueckert, D. A deep cascade of convolutional neural networks for dynamic MR image reconstruction. *IEEE Trans. Med. Imaging* **37**, 491–503 (2018).
[31] Rawat, S., Rana, K. P. S. & Kumar, V. A novel complex-valued convolutional neural network for medical image denoising. *Biomed. Signal Process. Control* **69**, 102859 (2021).
[32] Zhang, J., Niu, Y., Shangguan, Z., Gong, W. & Cheng, Y. A novel denoising method for CT images based on U-net and multi-attention. *Comput. Biol. Med.* **152**, 106387 (2023).
[33] Wang, J., Tang, Y., Wu, Z., Du, Q., Yao, L., Yang, X. & Zheng, J. A self-supervised guided knowledge distillation framework for unpaired low-dose CT image denoising. *Comput. Med. Imaging Graph.* **107**, 102237 (2023).
[34] Tajima, T., Akai, H., Yasaka, K., Kunimatsu, A., Yamashita, Y., Akahane, M. & Kiryu, S. Usefulness of deep learning-based noise reduction for 1.5 T MRI brain images. *Clin. Radiol.* **78**, e13–e21 (2023).
[35] Rajesh, C. & Kumar, S. An evolutionary block based network for medical image denoising using differential evolution. *Appl. Soft Comput.* **121**, 108776 (2022).
[36] Shi, P., Guo, L., Cui, H. & Chen, L. Geometric consistent fuzzy cluster ensemble with membership reconstruction for image segmentation. *Digit. Signal Process.* **134**, 103901 (2023).
[37] Cui, Y., Huang, H., Liu, J., Zhao, M., Li, C., Han, X., Luo, N., Gao, J., Yan, D.-M., Zhang, C., Jiang, T. & Yu, S. FFCM-MRF: An accurate and generalizable cerebrovascular segmentation pipeline for humans and rhesus monkeys based on TOF-MRA. *Comput. Biol. Med.* **170**, 107996 (2024).
[38] Wei, T., Wang, X., Li, X. & Zhu, S. Fuzzy subspace clustering noisy image segmentation algorithm with adaptive local variance & non-local information and mean membership linking. *Eng. Appl. Artif. Intell.* **110**, 104672 (2022).
[39] Song, S., Jia, Z., Shi, F., Wang, J. & Ni, D. Adaptive fuzzy weighted C-mean image segmentation algorithm combining a new distance metric and prior entropy. *Eng. Appl. Artif. Intell.* **131**, 107776 (2024).
[40] Bose, A., Maulik, U. & Sarkar, A. An entropy-based membership approach on type-II fuzzy set (EMT2FCM) for biomedical image segmentation. *Eng. Appl. Artif. Intell.* **127**, 107267 (2024).
[41] Luo, T.-J., Angadi, S. & Elashiri, M. A. Ensemble strategies exploration for the calibration data optimized spatial filters based SSVEP recognition algorithms. *Biomed. Signal Process. Control* **99**, 106932 (2025).
[42] Wang, Q., Zhuge, X., Yang, X. & Zhang, W.-A. Progressive Gaussian filtering for nonlinear uncertain systems based on Gaussian process models. *Signal Process.* **230**, 109801 (2025).
[43] Abolé, Y., Oboué, S. I., Chen, Y., Fomel, S., Zhong, W. & Chen, Y. An advanced median filter for improving the signal-to-noise ratio of seismological datasets. *Comput. Geosci.* **182**, 105464 (2024).
[44] Agyemang, E. F. A Gaussian Process Regression and Wavelet Transform Time Series approaches to modeling Influenza A. *Comput. Biol. Med.* **184**, 109367 (2025).
[45] Feltner, L., Stumpf, D. & Mort, P. On the use of the Fourier transform to determine contact curvature distributions in additive manufacturing powders. *Powder Technol.* doi: 10.1016/j.powtec.2025.120618 (2025).
[46] Choi, J., Hur, T., Park, D. K., Shin, N.-Y., Lee, S.-K., Lee, H. & Han, S. Early-stage detection of cognitive impairment by hybrid quantum-classical algorithm using resting-state functional MRI time-series. *Knowl.-Based Syst.* **310**, 112922 (2025).
[47] Li, L., Yang, W., Bai, S. & Ma, Z. KNN-GNN: A powerful graph neural network enhanced by aggregating K-nearest neighbors in common subspace. *Expert Syst. Appl.* **253**, 124217 (2024).
[48] Thakur, N., Kumar, P. & Kumar, A. Multilevel semantic segmentation and optimal feature selection based convolution neural network (Op-CNN) for breast cancer identification and classification using mammogram images. *Biomed. Signal Process. Control* **103**, 107374 (2025).
[49] Khan, S. & Kumar, V. A novel hybrid GRU-CNN and residual bias (RB) based RB-GRU-CNN models for prediction of PTB Diagnostic ECG time series data. *Biomed. Signal Process. Control* **94**, 106262 (2024).
[50] Velayudham, A., Kumar, K. M. & Priya, M. K. Improving brain MRI denoising using convolutional AutoEncoder and sparse representations. *Expert Syst. Appl.* **263**, 125711 (2025).
[51] Chen, Q., Ye, A., Ye, G., Huang, C. wearing myopia glasses on GANs: mitigating bias for pre-trained generative adversarial networks via online prior perturbation. *Applied Soft Computing*, **166**, 112133 (2024).
[52] Ding, W., Lei, B., Duan, C., Zhang, Q. grout diffusion model for single fractures in rock considering influences of grouting pressure and filling rate. *Tunnelling and Underground Space Technology*, **158**, 106392 (2025).
[53] Liu, W., Yu, H., Wang, Y., Liu, B., Tao, D., Chen, H. IW-ViT: independence-driven weighting vision transformer for out-of-distribution generalization. *Pattern Recognition*, **161**, 111308 (2025).

[54] Wang, B., Liang, Y., Cai, L., Huang, H., Zeng, H. image re-identification: where self-supervision meets vision-language learning. *Image and Vision Computing*, **154**, 105415 (2025).

[55] Liu, G., Zhao, Z., Li, C., Yu, Y. LeDA-GNN: learnable dual augmentation for graph neural networks. *Expert Systems with Applications*, **268**, 126288 (2025).

[56] Li, Y., Pan, L., Peng, Y., Li, X., Wang, X., Qu, L., Song, Q., Liang, Q., Peng, S. application of deep learning-based multimodal fusion technology in cancer diagnosis: a survey. *Engineering Applications of Artificial Intelligence*, **143**, 109972 (2025).

[57] Ge, Q., Xu, D., Cai, Q., Zhang, G., Zhou, S., Li, J., Xu, L. double filter noise reduction algorithm optimized by RBF neural network for laser absorption spectroscopy. *Infrared Physics & Technology*, **145**, 105718 (2025).

[58] Luo, Y., Li, J., Yang, J., Yan, S., Bai, Y., Zhang, X. adaptive filtering algorithm based on beta fluctuation and fractional order differential evolution in impulsive noise. *Engineering Applications of Artificial Intelligence*, **142**, 109937 (2025).

[59] Yuan, W., Liu, Y., Yan, Z., Pan, T. an improved Wiener filter-based method for identifying stall inception of transonic compressor. *Aerospace Science and Technology*, **155**(Part 1), 109576 (2024).

[60] Zhang, D., Zhang, Z., Chen, N., Wang, Y. dynamic convolutional time series forecasting based on adaptive temporal bilateral filtering. *Pattern Recognition*, **158**, 110985 (2025).

[61] Menagadevi, M., Mangai, S., Madian, N., Thiyagarajan, D. automated prediction system for Alzheimer detection based on deep residual autoencoder and support vector machine. *Optik*, **272**, 170212 (2023).

[62] Shu, Z., Entezari, A. RBP-DIP: residual back projection with deep image prior for ill-posed CT reconstruction. *Neural Networks*, **180**, 106740 (2024).

[63] Sengupta, S., Chyrmang, G., Bora, K., Das, H. S., Li, A., Lemos, B., Mallik, S. assessment of different U-Net backbones in segmenting colorectal adenocarcinoma from H&E histopathology. *Pathology - Research and Practice*, **266**, 155820 (2025).

[64] Massar, H., Stergiadis, C., Nsiri, B., Belhoussine Drissi, T., Klados, M. A. EMD-BSS: a hybrid methodology combining empirical mode decomposition and blind source separation to eliminate the ocular artifacts from EEG recordings. *Biomedical Signal Processing and Control*, **95**(Part A), 106475 (2024).

[65] Øveraas, H., Bryne, T. H., Johansen, T. A. a linear time-invariant Kalman filter for estimating height in the presence of ocean waves. *Ocean Engineering*, **320**, 120214 (2025).

[66] Li, G., Xie, J., Zhang, L., Cheng, G., Zhang, K., Bai, M. dynamic graph consistency and self-contrast learning for semi-supervised medical image segmentation. *Neural Networks*, **184**, 107063 (2025).

[67] Baciu, D. C. neural networks through the lens of evolutionary dynamics. *BioSystems*, 105386 (2025).

[68] Meng, X., Bachmann, M., Yang, F., Rethmeier, M. toward prediction and insight of porosity formation in laser welding: a physics-informed deep learning framework. *Acta Materialia*, **286**, 120740 (2025).

[69] Cao, Y., Li, Q., Ding, H., Xu, M., Tian, R., Bu, X. infrared attitude measurement signal parameter estimation based on gradient zero-crossing method. *Infrared Physics & Technology*, **145**, 105716 (2025).

[70] Yang, J., Gao, S., Zhao, X., Li, G. linear and nonlinear filters based on statistical similarity measure for sensor network systems. *Journal of the Franklin Institute*, **362**(1), 107412 (2025).

[71] He, J., Peng, B., Wang, G. a non-linear non-Gaussian filtering framework based on the Gaussian noise model jump assumption. *Automatica*, **178**, 112360 (2025).

[72] Zhang, Q., Huang, C., Yang, L., Yang, Z. salt and pepper noise removal method based on graph signal reconstruction. *Digital Signal Processing*, **135**, 103941 (2023).

[73] Yu, X., Peng, Y., Lou, P., Huang, B. poisson noise removal based on non-convex hybrid regularizers. *Journal of Computational and Applied Mathematics*, **457**, 116289 (2025).

[74] Jia, W., Jiao, Z., Zan, W., Zhu, W. probability density of the solution to nonlinear systems driven by Gaussian and Poisson white noises. *Probabilistic Engineering Mechanics*, **77**, 103658 (2024).

[75] Milotti, V., Favaro, G., Granata, M., Forest, D., Michel, C., Teillon, J., Lemaître, A. thermal noise reduction in ion-beam sputtered HfO_2:Ta_2O_5 thin films via high-temperature treatment. *Optical Materials*, **163**, 116901 (2025).

[76] Nouri, M., Shayesteh, M. G., Farhangian, N. chromatic dispersion and nonlinear phase noise compensation based on KLMS method. *Optics Communications*, **351**, 149–154 (2015).

[77] Naccache, F., Hamdi, M.-A., Chazot, J.-D., Anciant, M. semi-analytical model of noise transmission through finite length cylinder with poroelastic core using Biot's and Shell theories. *Journal of Sound and Vibration*, **535**, 117102 (2022).

[78] Zamponi, R., Rubio Carpio, A., Avallone, F., Ragni, D. noise source analysis of porous fairings in a scaled landing gear model. *Aerospace Science and Technology*, **158**, 109885 (2025).

[79] Boughaba, N. E. H., Bouzid, B., Yahlali, N. assessment of Cerenkov optical noise in a brachytherapy scintillating fibre dosimeter with an air-core Ag-PTFE light guide. *Radiation Measurements*, **181**, 107348 (2025).

[80] [Zhang, W., Song, P., Bai, Y., Geng, H., Wu, Y., Zheng, Z. non-systematic noise reduction framework for ToF camera. *Optics and Lasers in Engineering*, **180**, 108324 (2024).

[81] Wu, X., Huang, D. a local local oscillator passive continuous variable quantum key distribution scheme with trusted phase noise model and optical amplifiers. *Optics Communications*, **584**, 131796 (2025).

[82] Gómez-Catasús, J., Barrero, A., Llusia, D., Iglesias-Merchan, C., Traba, J. wind farm noise shifts vocalizations of a threatened shrub-steppe passerine. *Environmental Pollution*, **303**, 119144 (2022).

[83] López-Hernández, J., Vázquez-Medina, R., Ortiz-Moctezuma, M. B., Del-Rio-Correa, J. L. digital implementation of a pseudo-random noise generator using chaotic maps. *IFAC Proceedings Volumes*, **45**(12), 209-214 (2012).

[84] Li, J., Chen, Y., Li, Y., Feng, Q. DAS seismic signal recovery with non-uniform noise based on high-low level feature fusion model. *Journal of Applied Geophysics*, **229**, 105481 (2024).

[85] Marcu, A., Nicolae, I., Viespe, C. active surface geometrical control of noise in nanowire-SAW sensors. *Sensors and Actuators B: Chemical*, **231**, 469-473 (2016).

[86] Jamali, S. S., Mills, D. an assessment of intrinsic noise of pseudo-reference electrodes and instrumental noise to enable reliable electrochemical noise measurements in situ on organically coated metal. *Electrochimica Acta*, **398**, 139279 (2021).

[87] Li, R., Jiao, N., An, B., Wang, Y., Li, W., Chen, L., Tian, L., Zheng, Y. optimizing frequency noise calibration and manipulation in an

active feedback control loop. *Optics & Laser Technology*, **174**, 110617 (2024).

[88] Katkar, R., Steffy, D. D., Noujeim, M., Deahl II, S. T., Geha, H. the effect of milliamperage, number of basis images, and export slice thickness on contrast-to-noise ratio and detection of mandibular canal on cone beam computed tomography scans: an in vitro study. *Oral Surgery, Oral Medicine, Oral Pathology and Oral Radiology*, **122**(5), 646-653 (2016).

[89] Kumar, A., Gupta, T. K., Shrivastava, B. P., Gupta, A. impact of temperature variation on noise parameters and HCI degradation of recessed source/drain junctionless gate all around MOSFETs. *Microelectronics Journal*, **134**, 105720 (2023).

[90] Moniri, Z., Babaei, A., Parsa Moghaddam, B. robust numerical framework for simulating 2D fractional time–space stochastic diffusion equation driven by spatio-temporal noise: L1-FFT hybrid approach. *Communications in Nonlinear Science and Numerical Simulation*, **146**, 108791 (2025).

[91] Zhao, H., Gallo, O., Frosio, I., Kautz, J. loss functions for image restoration with neural networks. *IEEE Transactions on Computational Imaging*, **3**(1), 47-57 (2017).

[92] Darvishi, O., Maihami, V., Khamforoosh, K. improvement of the fuzzy clustering algorithm for medical image segmentation and denoising using fast bilateral filtering. *Contemporary Mathematics*, **622**, 6512 (2025).